International Journal of Innovative Environmental Studies Research 10(1):103-114, Jan.-Mar., 2022

© SEAHI PUBLICATIONS, 2022 www.seahipaj.org ISSN: 2354-2918

Structural Mapping And Sedimentary Thickness Determination Of Bornu Basin Using Source Parameter Imaging Technique

Gladman, Goteh B., Nwankwo, Cyril N. & Emujakporue, Godwin O.

University of Port Harcourt, Port Harcourt, Nigeria

ABSTRACT

Aeromagnetic data is a tool deployed in delineating regional basement structures, depths and sedimentary thickness in frontier basin. The aeromagnetic data of the Bornu region was interpreted to delineate its structural framework, as well as the depth to magnetic basement that could support accumulation of economic minerals. The acquired data was subjected to different enhancement techniques which include: First vertical derivative (FVD), total horizontal derivative (THDR), analytical signal filter (ASF), center to exploratory targeting (CET) as well as depth estimation method of source parameter imaging (SPI). Results from analytical signal and CET, delineated and enhanced the magnetic signatures that reflect the structural features of the area showing lineaments along NE-SW, ENE-WSW and WNW-ESE major trends and NW-SE, NNE-SSW, NNW-SSE minor trends, with evident ENE-WSW and NE-SW trends as most dominant in the area. The result from SPI revealed a depth range between 1101.3 m (shallow magnetic source bodies) and 39607.1 m (deep-seated magnetic source bodies). The maximum depths obtained from this estimation method are theoretically sufficient for hydrocarbon accumulation.

Keywords: aeromagnetic data, magnetic signatures, structural framework, source parameter imaging, sedimentary thickness

INTRODUCTION

The aeromagnetic method of geophysical investigation has been employed across the Chad (Bornu) Basin and Nigeria at large for delineating tectonic structures which could be potential hosts for various mineral deposits and their host rocks. Magnetic method play a major role in mapping out structures such as faults, contacts, folds, intrusions and shear zones for the detection of mineralized deposits. The magnetic survey aims at probing the Earth's internal structures as a result of changes in the magnetic field that occur due to magnetic properties of rocks under the Earth's surface.

Aeromagnetic surveys play a vital role in understanding the basement morphology and tectonic evolution of sedimentary basins. The aeromagnetic data are an effective cost-effective geophysical tool deployed in basin exploration to delineate subsurface geological features, infer the prevailing fault patterns and determine the basement depth (Saibi *et al*., 2016). The propagation of the basement structures into the overlying sediment might aid fluid flow and fault-dependent hydrocarbon reservoirs associated with oil and gas fields (Ali *et al*., 2013). Sedimentary basins are often associated with weak magnetic response as a result of the low magnetic susceptibility sediments present in them. Thus, mapping the basement-sediment interface presents enhanced images about the basement geometry and variations in the thickness of sediments (Oladele *et al*., 2016).

Structural characterization and depth estimation of the Bornu Basin has been carried out by numerous researchers using various geophysical methods; Sanusi and Likkason (2016) carried out a detailed analysis of total-field aeromagnetic data over the entire western half of the Bornu Basin and its adjoining areas using angular spectral analysis, upward continuation and low-pass filtering to accentuate the effects

of deep-seated structures within the area. Superposition of the inferred regional lineaments on the surface geology suggests that the inferred lineaments exerted structural control on the sedimentation pattern of the area. Spectral depth analysis of aeromagnetic data covering part of Chad Basin was undertaken by Adewumi *et al*. (2017) to estimate its sedimentary thickness. An average sedimentary thickness of 3.35 km, thought to be sufficient for hydrocarbon presence, was observed in their research. Lawal and Nwankwo (2017) evaluated the depth to the bottom of magnetic sources and heat flow from high resolution aeromagnetic data of part of Nigeria sector of the Chad Basin. The obtained result varies between 18.18 and 43.64 km. Also the heat flow parameters vary between 33.23 and 79.76 mW/m^2, while the geothermal gradient vary from 13.29 to 31.90 °C/km respectively.

This present study aims at the structural interpretation of aeromagnetic data of Bornu Basin to give further insight into the basement rock pattern, basin architecture, thickness of sediments using the Source Parameter Imaging (SPI) technique, as well as the features that could be trapped for hydrocarbon-bearing formation. The Source Parameter Imaging (SPI) of aeromagnetic fields over the area would differentiate and characterize regions of deep magnetic Basement (sources) from those of shallow magnetic basement and also to determine the depths to the magnetic sources.

Geology and Location of Study Area

The study area is bounded by latitude 12° to 13°N and longitude 12’30° to 13’30°E within parts of Chad Basin, Nigeria (Figure 1.1). The Nigerian sector of the Chad Basin, locally known as the Bornu Basin, is one of Nigeria’s inland basins located in north eastern Nigeria. It covers about one-tenth of the total area of the Chad Basin, which is a regional large structural depression common to five countries (Cameroon, Central African Republic, Chad, Niger and Nigeria). The main structures are basement – involved and detached faults and simple symmetrical folds with NE-SW, NW-SE and E-W trends. The basin contains marine and continental sediments comprising the Bima Sandstone at the bottom, Gongila Formation, Fika Shale, Kerri-Kerri and Chad Formations (Obaje, 2009)**.** The basin is generally composed of feldspathic, coarse grained sandstones, with beds of quartz pebbles, siltstones, fossiliferous limestone beds, diatomite, clays and some layers of shale. (Okosun, 1995).

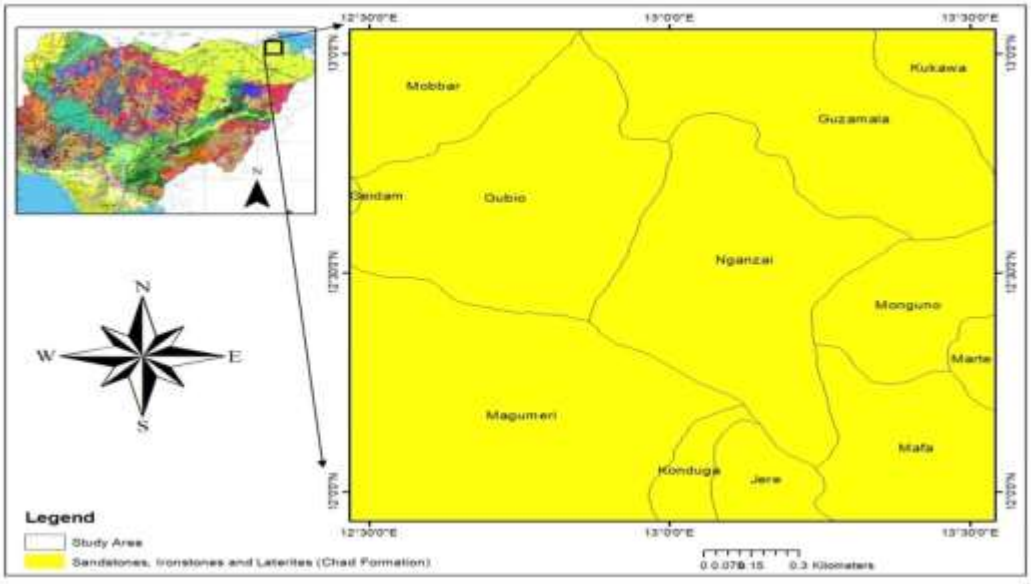

Figure 1 Geological map of the study area (Adapted from NGSA)

MATERIALS AND METHOD

Nature and Source of Data

The survey of the area of study was carried between the years 2005 and 2009 by Fugro for Nigeria geological survey agency (NGSA). The data were obtained at an altitude of 0.10 km terrain clearance along a parallel traverse line spacing of 0.5 km oriented in NW-SE, with an azimuth of 135° and a tie line spacing of 2 km in NE-SW direction, with an azimuth of 45° from the true north. The geomagnetic gradient was removed from the data using the International Geomagnetic Reference Field (IGRF) formula for 2005. The data were then interpolated into rectangular grids to generate the total magnetic intensity (TMI) grid. Each TMI map is on a scale of 1:100,000 and half-degree sheets, covering an area of about 65x65 km^2 contoured mostly at 10 nT intervals. The high resolution aeromagnetic data of Gazubure (sheet 44), Dububali (sheet 45), Gubio (sheet 66) and Masu (sheet 67) used for this study were obtained from the NGSA and merged into a single TMI grid. The TMI map provided the basis for consequent application of enhancement filters required for detailed structural interpretation of the area under study. The Software application employed to interpret/analyze the data are the Oasis Montaj and the Surfer.

Data Analysis and Interpretation techniques

The data processing started with producing the Total Magnetic Intensity (TMI) map by adopting line gridding method, with further data enhancement method of separating the regional field from the total magnetic intensity field to obtain a residual data, using the first order polynomial fitting of least square method. Structural enhancement filters were then applied to the grid to locate edges and contacts of linear features. The edge detection method employed in this study include first vertical derivative (FVD), total horizontal derivative (THDR), analytic signal (AS) filter and centre to exploratory targeting (CET). Lineament extracted from the resultant maps were analyzed to infer the prevalent tectonic trends in the study area. Depths to magnetic sources were determined using the source parameter imaging (SPI) method.

First Vertical Derivative (FDV): This filtering transformation was executed on the aeromagnetic data so as to make more apparent the shallow related magnetic bodies. The filtering process is governed by the equation:

$$\mathcal{F}\left[\frac{d^n \emptyset}{dz^n}\right] = K^n \mathcal{F}(\emptyset) \qquad 1$$

where n = 1, the nth order vertical derivative, Ø = field potential and $\mathcal{F}$ = Fourier transform.

Total Horizontal Derivative (THDR): As suggested by Verduzco *et al*. (2004), the total horizontal derivative (THDR) used for edge detection can be given by

$$THDR = \sqrt{\left(\frac{\partial M}{\partial x}\right)^2 + \left(\frac{\partial M}{\partial y}\right)^2} \qquad 2$$

where $\left(\frac{\partial M}{\partial x}\right)$ and $\left(\frac{\partial M}{\partial y}\right)$ are the horizontal derivatives of the magnetic field. A tabular body generates total horizontal derivative which tends to overlie the edges of the anomalous body, whether horizontal or vertical, and separated apart (Cordell and Grauch, 1985). The THDR is a good detector of shallow linear features since it only computes the first horizontal derivatives of the field in the x and y directions (Cooper and Cowan, 2008). The THDR was used in this study to enhance edges of near-surface structures like faults and fracture zones.

Analytic Signal Filter (ASF)

The analytic signal filter which generates a calculated magnetic anomaly improved map, that define edges (boundaries) of geological anomalous magnetization distribution, actually takes the magnitude of the

square root of the vertical and horizontal components of the magnetic responses (Philips, 2000). The application of the analytic signal (total gradient) method gives good horizontal locations for structures independent of their magnetic latitude (Azizi *et al*., 2015). The method of analytic signal uses the derivatives of the magnetic field independent of the angles of strike, dip, inclination, declination and remanent magnetization (Debeglia and Corpel, 1997).

According to Roest *et al*. (1992), the amplitude of the three-dimensional analytic signal at location (x, y, z) can be obtained from the three orthogonal gradients of the total magnetic field using the equation:

$$|A(x,y,z)| = [(\frac{dT}{dx})^2 + (\frac{dT}{dy})^2 + (\frac{dT}{dz})^2]^{1/2} \quad 3$$

where $|A(x,y,z)|$ is the amplitude of the analytic signal at (x, y, z), T is the observed magnetic field at (x, y, z).

Center to Exploratory Targeting (CET)

This procedure adopts the method of identifying linear structures within the aeromagnetic data through repeated map by-product forms that include standard deviation which determines magnetic variations, then phase symmetry to separate laterally continuous lines. Equation (4) below was adopted as the algorithm (Kovesi, 1991).

$$\sigma = \sqrt{\frac{1}{N}\sum_{i=1}^{N}(x_i - \mu)^2} \quad 4$$

Afterward, the resultant lineaments are enhanced by suppressing noise and background signals using an amplitude thresholding.

Source Parameter Imaging (SPI)

The SPI technique developed by Thurston and Smith (1997), which shows depths, susceptibility contrasts, edge locations, and dips, utilizes the relationship between source depth and the local wave number (*K*) of the observed field. The technique is that the inverse of depth is defined by the peaks of the local wavenumber for vertical contacts. The equation (5) below was the algorithm developed in calculating the source depth.

$$Depth = \frac{1}{K_{max}} \quad 5$$

where K_{max} is the peak value of the local wavenumber K over the steep source.

The SPI map provides a better image of the basement-sediment interface. It was employed in this study to determine the depth to the causative sources.

RESULTS AND DISCUSSIONS

The total magnetic intensity (TMI) map is produced in different colours, with green to blue colour depicting low magnetic anomalies while red to pink colour depicts high anomalies. The total magnetic intensity map (Figure 2) of the study area exhibits magnetically heterogeneous (high and low) anomalies ranging from -70.4 to 228.1 nT. The variations in magnetic field intensity can be attributed to the changes in depth, magnetic susceptibility differences, degree of strike, angle of dip, plunge and lithology (Obiora *et al*., 2015). The lower portion of the area is predominantly of high anomaly while the upper part is dominated by low magnetic anomalies. Short wavelength anomalies with high frequency of occurrence are observed to dominate the North-eastern corner.

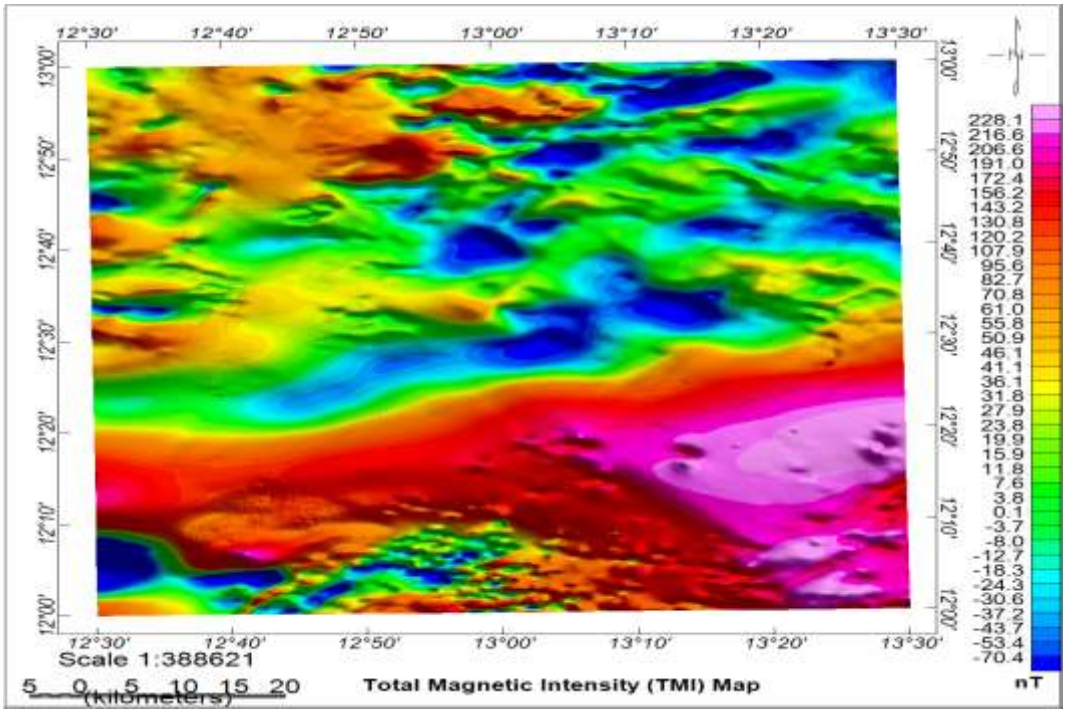

Figure 2 Total magnetic intensity (TMI) map of the study area

The 2D residual aeromagnetic map (Figure 3) of the area reveals anomalies with values ranging between -77.6 to 65.6 nT, thus suggesting the area contains predominantly high residual anomalies and small portion of low residual magnetic anomalies. This indicates the presence of intrusive bodies in the area. High magnetic anomalies are observed in the eastern, southeastern, western and southwestern axes. This could be attributed to subsurface rock containing large magnetic response (Oghuma *et al.*, 2015). Low values of magnetic anomalies appear from the southern region through the central portion to the northern part of the map. This could be likely due to the presence of weak magnetic sources or sedimentary rocks (likely sandstone) in the area. Sedimentary rocks usually give low magnetic response (Clark, 1997). The residual map and TMI map exhibits similar features.

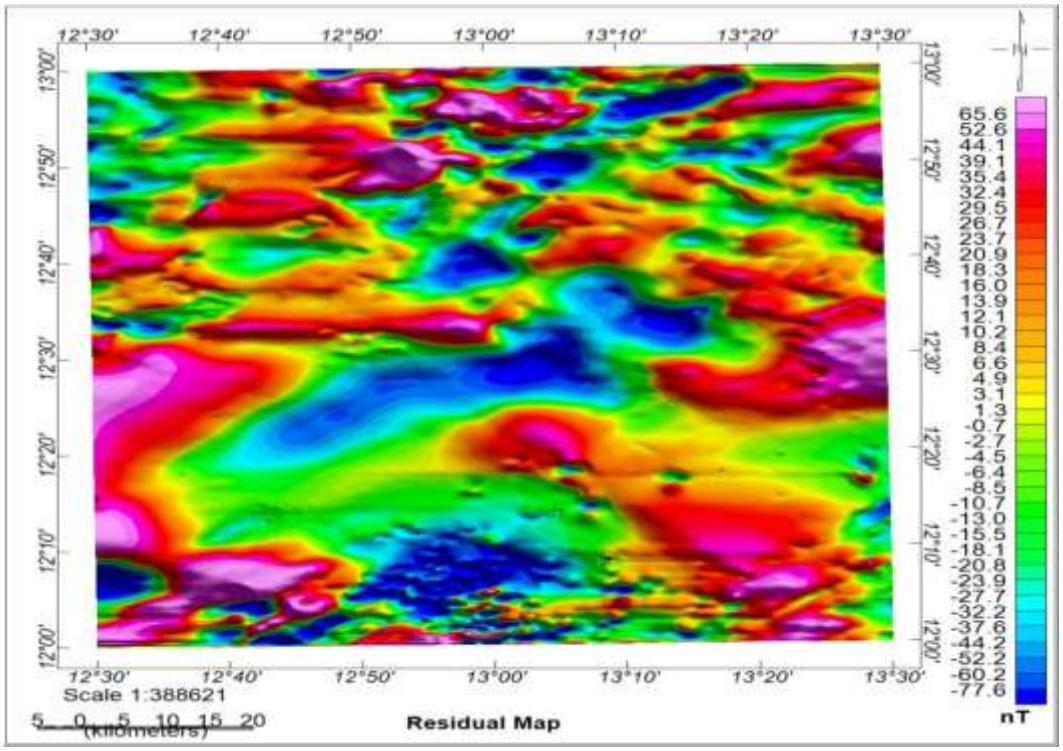

Figure 3. The 2D residual map of the study area

The first vertical derivative map (Figure 4) enhances shallow geologic sources within the area and gives a good representation of near surfaces structures such as structural lineaments (faults and joints) and igneous intrusions that could be associated with mineralization systems in the area and determines the precise border between lithological units. Magnetic anomalies of values varying from -0.047 to 0.037 nT/m are observed on the FVD map. The northern and southern regions in the study area as characterized by magnetic highs also correspond to regions with high fracture density and having fractures generally trending NE-SW and NW-SE; these likely represent dykes, sills, faults, joints, etc. The patterns and shapes of the curvilinear nature of some of the features observed at the northern part of the area under study might represent undulating folds which can serve as structural traps for hydrocarbon maturation within the study area.

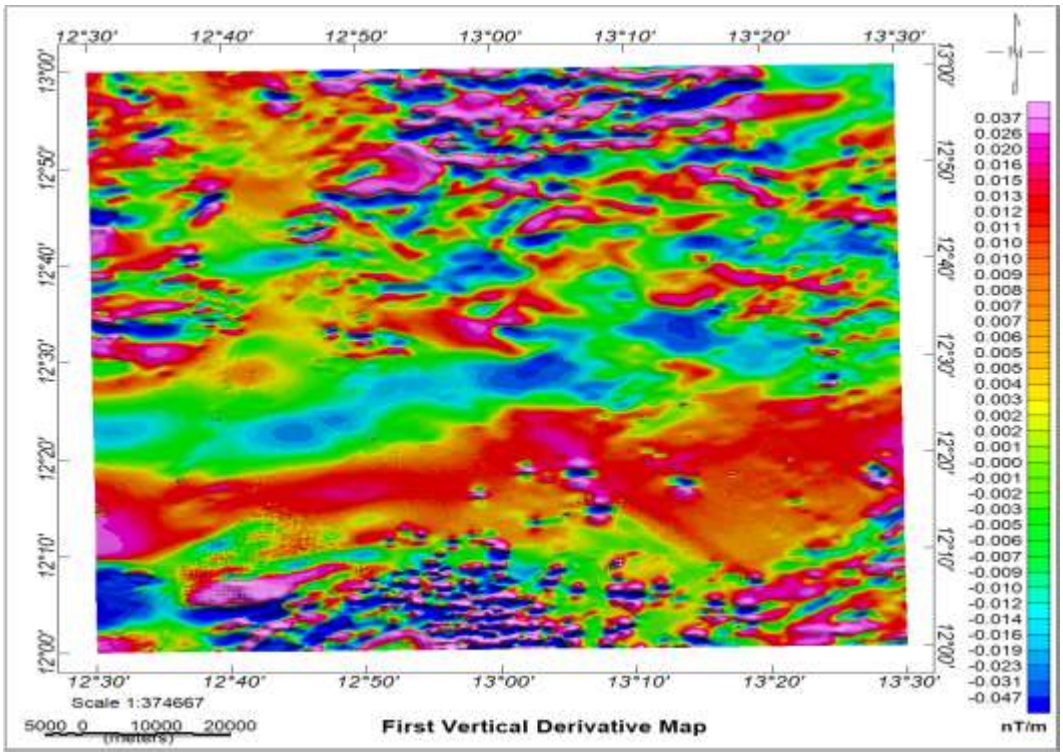

Figure 4 The first vertical derivative (FVD) map of the study area

The horizontal derivative field (Figure 5 and Figure 6) locates and maps the major anomalies within the study area as a measure of the degree of distortion to the magnetic signatures. Observation of the derivative maps reveal that the derivative in the x-direction intensifies anomalies trending in the x-direction while that in the y-direction enhances the features trending in the y-direction. The first horizontal derivative (x-direction) map (Figure 5) has magnetic anomalies ranging from -0.018 to 0.018 nT/m, while the second horizontal (y-direction) map (Figure 6) has anomaly values ranging from -0.038 to 0.039 nT/m. The effect of basement features showing linear structure with an averagely high susceptibility with short wavelenghts can be delineated in the northern and southern part of the study area thereby indicating shallow sedimentation. Major structures delineated on the two maps trend NE-SW, NW-SE and E-W, corresponding to the ones observed on the vertical derivative maps.

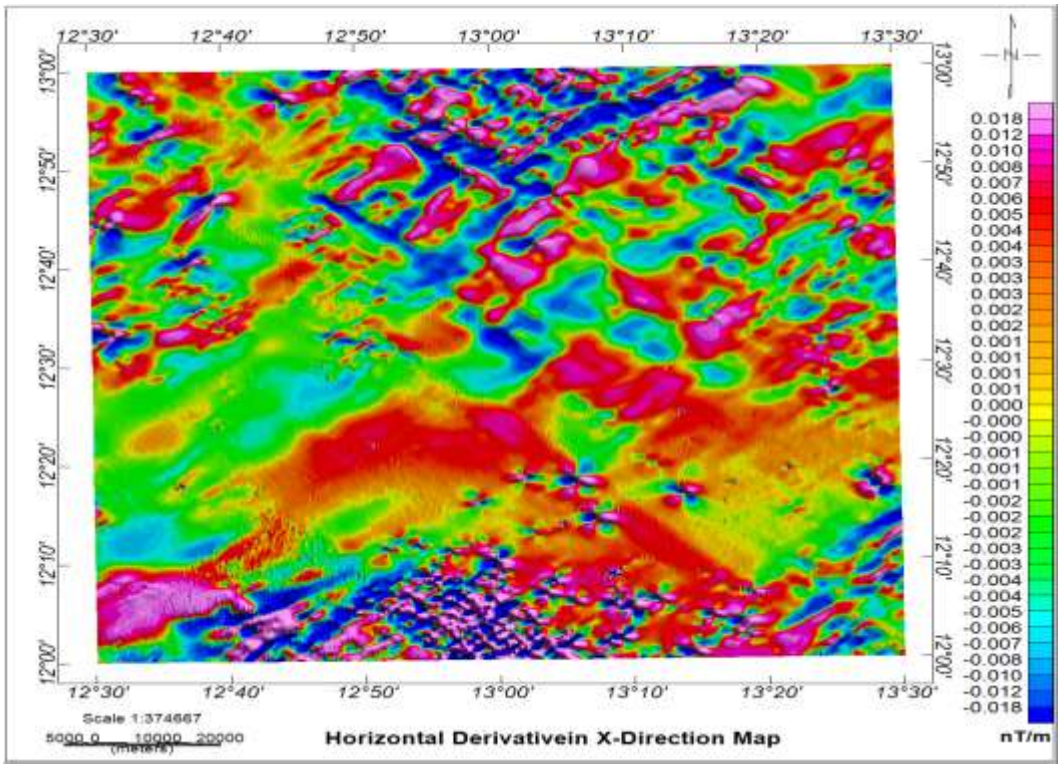

Figure 5 First Horizontal Derivative (X-direction) Map

The analytical signal map (Figure 7) exposes the variations in amplitudes of the magnetic anomalies which help in delineating the study area into regions of outcrop, intermediate structures and basement under the influence of thick sedimentation. Three regions can be clearly observed; regions whole amplitude responses are high ranging from 0.022 to 0.085 nT/m which could be made up of sandstone, ironstone and laterite (Figure 1) at the northern and southern

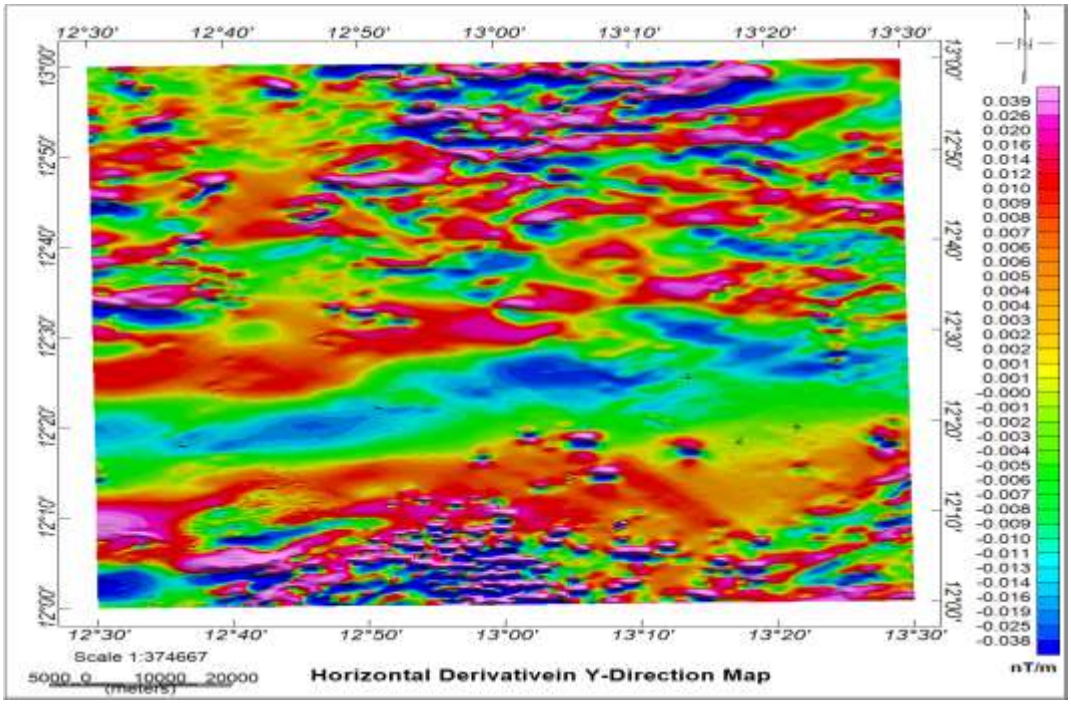

Figure 6 Second Horizontal Derivative (Y-Direction) Map

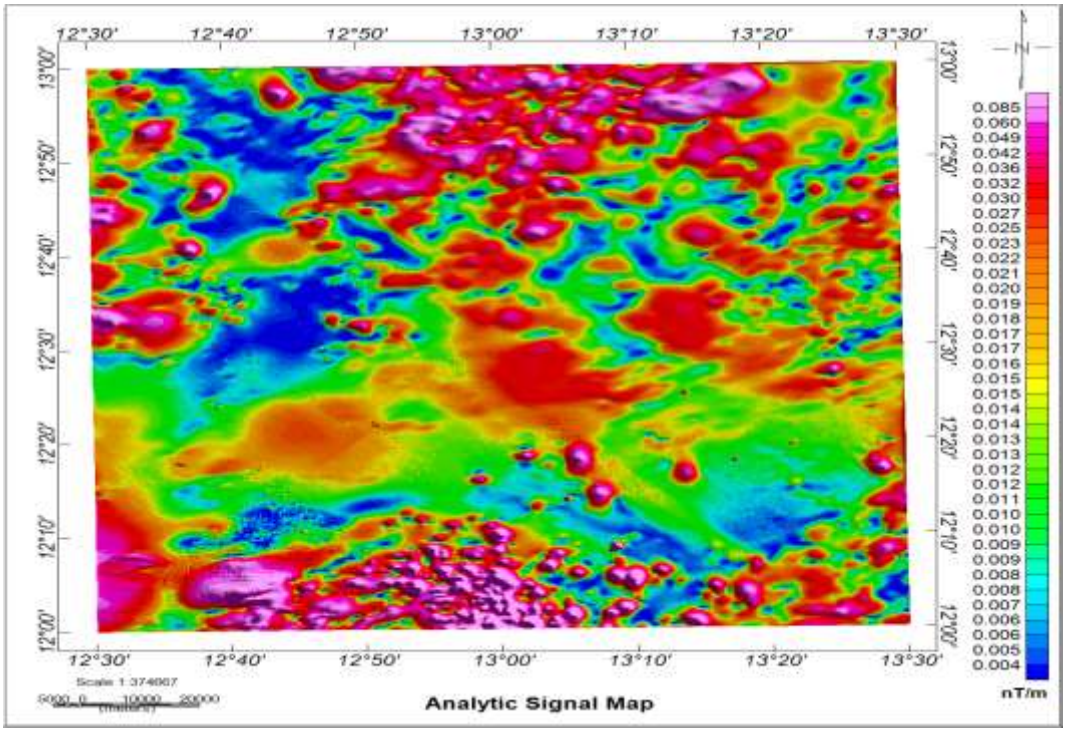

Figure 7 Analytical signal map

parts of the study area; regions of intermediate (between high and low) ranging from 0.014 - 0.018 nT/m and regions whose amplitude are low ranging from 0.004 - 0.012 nT/m, which represents regions with relatively good sedimentation at the central part of the study area.

The lineaments exhibited by the vectorization map (Figure 8) reveal the rocks (likely sandstone and ironstone)(Figure 1) that occupy the northern and southern parts of the study area are highly deformed as

compared with the central part covered by cretaceous sedimentation. The lineament map reveals that the most prominent lineaments delineated trend NE-SW, NW-SE, NNE-SSW and NNW with few traces of N-S direction.

The Basement depth determination via employing the Source Parameter Imaging (SPI) method reveals depth variations to different anomalous sources and thickness of sediments across the basin. A clear image of the rugged topography of the basement is revealed on the SPI map (Figure 9). The estimated depth result for the aeromagnetic data varies from 1005.48m (shallow magnetic anomalous bodies) to 3962.93m (deep lying magnetic anomalous bodies).

Two major basement depressions (mini-basins) were mapped in the area, and are located at the western and eastern parts of the study area. The basement uplifts in the area influenced the faulting and trapping mechanisms. The sedimentary thickness (3.9 km) in the area is given by the estimated depth to basement in the mini-basins. The depth range obtained in this study is in close agreement with earlier values obtained in the basin by other researchers (Okonkwo *et al*., 2012; Aderoju *et al*., 2016).

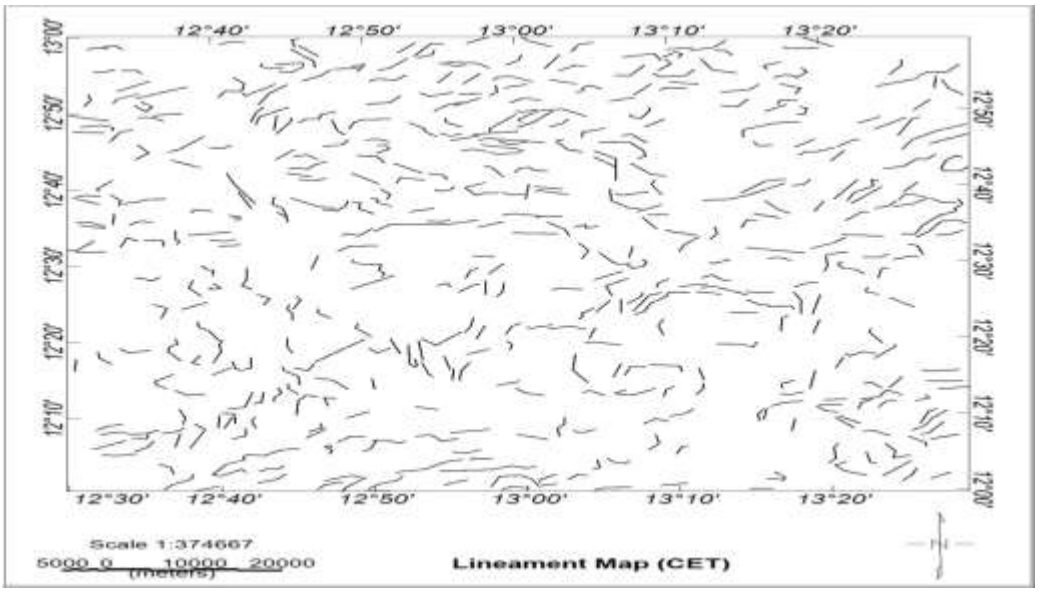

Figure 8. Center to exploratory targeting (CET) map showing the lineaments in the study area

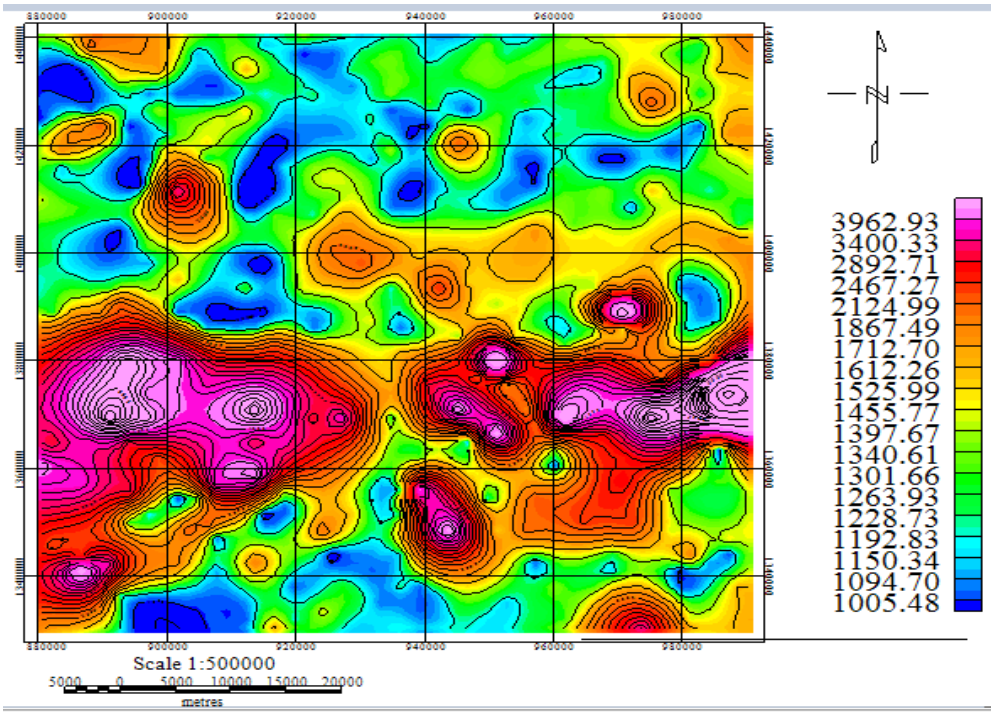

Figure 9. Source Parameter Imaging (SPI) aeromagnetic map

The presence of shallow and deep-seated structures can be attributed to the occurrence of faults and fracture networks, with significant trends in the NE-SW, NW-SE, NNE-SSW and NNW directions and few traces of N-S direction. The estimated depth to basement of 3.9 km in thickness of sediments in the basin is considered to be sufficient for hydrocarbon accumulation. These features gave an insight into understanding the geological settings of the area.

CONCLUSIONS

The aeromagnetic data covering parts of the Bornu Basin have been analyzed and interpreted qualitatively and quantitatively in details. Variations between high and low anomalies in the area as revealed in the magnetic signatures on the maps, indicate variations in the magnetic susceptibility of the underneath basement and sedimentary rocks.

REFERENCES

Aderoju, A. B., Ojo, S.B., Adepelumi, A. A. and Edino, F. (2016): A Reassessment of Hydrocarbon Prospectivity of the Chad Basin, Nigeria, using Magnetic Hydrocarbon Indicators from High Resolution Aeromagnetic Imaging. Ife Journal of Science, Vol. 18, No. 2.

Adewumi, T., Salako, K. A., Salami, M. K., Mohammed, M. A. and Udensi, E. E. (2017): Estimation of Sedimentary Thickness using Spectral Depth Analysis of Aeromagnetic Data over Part of Bornu Basin, Northeast, Nigeria. Asian Journal of Physics and chem. Sciences 2(1):1-8.

Ali, M. Y., Watts, A. B. and Farid, A. (2013) Gravity anomalies of the United Arab Emirates: implications for basement structures and infra-Cambrian salt distribution. GeoArab. 18(4)49-80.

Azizi, M., Saibi, H. and Cooper, G. R. J. (2015). Mineral and structural mapping of Aynak-Logar Valley (Eastern Afganistan) from hyperspectral remote sensing data and aeromagnetic data. Arab J. Geosci., 8, pp. 10911-10918.

Clark, D. A. (1997): Magnetic petrophysics and magnetic petrology: aids to geological interpretation of magnetic surveys. AGSO Journ. Australian Geology & Geophys. 17(2), 83-103.

Cooper, G. R. J. and Cowan, D. R. (2008). Edge enhancement of potential-field data using normalized statistics. Geophysics 73(3): 111-114.

Cordell, L. and Grauch, V. J. S. (1985). Mapping basement magnetization zones from aeromagnetic data in the San Juan Basin, New Mexico. In the Utility of Regional Gravity and Magnetic Anomaly Maps: Hinze WJ Ed. Society of Exploration Geophysicists: 181-197.

Debeglia, N. and Corpel, J. (1997). Automatic 3D interpretation of Potential Field Data Using Analytic Signal Derivatives. Geophysics, 62, 87-96.

Kovesi, P. (1991) Image features from phase congruency. Journal of Computer Vision Res. 3:55.

Lawal, T. and Nwankwo, L. (2017). Evaluation of the depth to the bottom of magnetic sources and heat flow from high resolution aeromagnetic (HRAM) data of part of Nigeria sector of Chad Basin. Arabian Journal of Geosciences. 10(17): 378.

Obaje, N.G. (2009): The Bornu Basin (Nigerian Sector of the Chad Basin). In: Geology and Mineral Resources of Nigeria. Lecture Notes in Earth Sci., vol 120. Springer, Berlin, Heidelberg.

Obiora, D. N., Ossai, M. N. and Okwohi, E. (2015): A case study of aeromagnetic data interpretations of Nsukka Area, Enugu State, Nigeria for hydrocarbon Exploration. Int. J. Phys. Sci, 10(17): 503-519.

Oghuma, A.A., Obiadi, I.I. and Obiadi, C.M. (2015). 2-D spectral analysis of aeromagnetic anomalies over parts Montu and Environs, Northeastern, Nigeria. *J. Earth Sci. Clim. Change* 6:8-14.

Okonkwo, C. C., Onwuemesi, A. G., Anakwuba, E. K., Chinwuko, A. I., Ikumbur, B. E. and Usman, A. O. (2012). Aeromagnetic interpretation over Maiduguri and Environs of Southern of Chad Basin, Nigeria. Journal of Earth Sciences and Geotechnical Engineering 2(3):77-93.

Okosun, E. A. (1995) Review of Geology of Bornu Basin. J. of Mining and Geol., 31, 113-122.

Oladele, S., Ayolabi, E. A. and Dublin-Green, C. O. (2016). Structural characterization of the Nigerian sector of the Benin basin using Geopotential field attributes. J. Afr. Earth Sci. Elsevier 121:200-209.

Philips, J. D. (2000). Locating magnetic contacts: a comparison of the horizontal gradient analytic signal, and local wavenumber methods. SEG Technical Program Expanded Abstracts, 2000, pp. 402-405.

Roest, W. R., Verhoef, J. and Pilkington, M. (1992). Magnetic interpretation using the 3-D analytic signal. Geophysics. Volume 57(1): 9-210. SEG-Library.

Saibi, H., Azizi, M. and Mogren, S. (2016). Structural investigations of Afghanistan deduced from remote sensing and potential field data. Acta Geophys.

Sanusi, Y. A. and Likkason, O.K. (2016): Angular Spectral Analysis and Lowpass Filtering of Aeromagnetic Data over Western Parts of Bornu Basin of Nigeria. Nigerian Journal of Basic and Applied Science, 24(2): 73-84.

Thurston, J. B. and Smith, R. S. (1997). Automatic conversion of magnetic data to depth, dip and susceptibility contrast using the SPI^{TM} method. Geophysics 62, 807-813.

Verduzco, B., Fairhead, J. D., Green, C. M. and MacKenzie, C. (2004). New insights into magnetic derivatives for structural mapping. Lead Edge 23: 116-119.